

# GUIDED FILTER BASED EDGE-PRESERVING IMAGE NON-BLIND DECONVOLUTION

Hang Yang, Ming Zhu

Changchun Institute of Optics, Fine Mechanics and Physics  
Chinese Academy of Science  
China, Changchun 130033  
yanghang09@mails.jlu.edu.cn  
mingzhuca@163.com

Zhongbo Zhang, Heyan Huang

Department of Mathematics  
Jilin University  
China, Changchun 130012  
zhongbozhang@jlu.edu.cn  
huanghy10@mails.jlu.edu.cn

## ABSTRACT

In this work, we propose a new approach for efficient edge-preserving image deconvolution. Our algorithm is based on a novel type of explicit image filter - guided filter. The guided filter can be used as an edge-preserving smoothing operator like the popular bilateral filter, but has better behaviors near edges. We propose an efficient iterative algorithm with the decouple of deblurring and denoising steps in the restoration process. In deblurring step, we proposed two cost function which could be computed with fast Fourier transform efficiently. The solution of the first one is used as the guidance image, and another solution will be filtered in next step. In the denoising step, the guided filter is used with the two obtained images for efficient edge-preserving filtering. Furthermore, we derive a simple and effective method to automatically adjust the regularization parameter at each iteration. We compare our deconvolution algorithm with many competitive deconvolution techniques in terms of ISNR and visual quality.

**Index Terms**— deconvolution, guided filter, regularization parameter.

## 1. INTRODUCTION

Image deconvolution is a classical inverse problem existing in a wide variety of image processing fields, including physical, optical, medical, and astronomical applications.

The degradation procedure is often modeled as the result of a convolution with a low-pass filter

$$y = \mathcal{H}u_{orig} + \gamma = h * u_{orig} + \gamma \quad (1)$$

where  $u_{orig}$  and  $y$  are the original image and the observed image, respectively.  $\gamma$  is generally assumed to be independent and identically distributed (i.i.d.) zero-mean additive white Gaussian noise (AWGN) with variance  $\sigma^2$ . " $*$ " denotes convolution, and  $h$  denotes the point spread function (PSF) of a linear time-invariant (LTI) system  $\mathcal{H}$ .

To find a unique and stable solution, a number of deconvolution algorithms have been proposed. In these meth-

ods, the Wiener filter and the constrained least squares algorithm, can solve this problem in the frequency domain in a fast speed. In [1], Neelamani *et al.* proposed an efficient, hybrid Fourier-wavelet regularized deconvolution (ForWaRD) algorithm. Transformations such as curvelets [2], shearlets [3] and wave atoms [4] are popular for image representation and are often used for image restoration. Another popular deconvolution method is based on total variation. Variations of this method have also been proposed in [5][6]. These methods are well known for its edge-preserving property, and can generally achieve state-of-the-art results. In particular, the SV-GSM [7] and the BM3D (Block Matching 3D) [8] are among the current best image deconvolution methods. There are many useful algorithms and additional techniques in references [9][10].

In this work, we adopt a different approach to the problem of image restoration by exploiting guided filter [11] to regularize the inverse problem. Derived from a local linear model, guided filter generates the filtering output by considering the content of a guidance image. We first integrate this filter into a iterative deconvolution method. The iterative process consists of two parts: deblurring and denoising. The output of the deblurring process are one noisier estimated image and a less noisy one. The former will be filtered and the latter will work as the guidance image respectively in denoising step. During the denoising process, the guided filter will be applied to the output of last step to reduce noise and refine the result of last step. Furthermore, regularization parameters play the important role in our method. We apply the discrepancy principle to automatically determine regularization parameters in each iteration. We demonstrate with experimental results that this algorithm provides competitive and even better figures of merit compared with state-of-the-art methods.

## 2. GUIDED IMAGE FILTERING

Guided filter was defined in [11][12]. Currently it is one of the fastest edge-preserving filters. Now, we introduce guided filter, which involves a guidance image  $u_I$ , an filtering input

image  $u_p$ , and an output image  $u$ . Both  $u_I$  and  $u_p$  are given beforehand according to the application, and they can be identical.

The key assumption of the guided filter is a local linear model between the guidance  $u_I$  and the filtering output  $u$ . We assume that  $u$  is a linear transform of  $u_I$  in a window  $\omega_k$  centered at the pixel  $k$  (the size of  $\omega_k$  is  $w \times w$ ):

$$u(i) = a_k u_I(i) + b_k \quad (2)$$

where  $(a_k, b_k)$  are some linear coefficients assumed to be constant in  $\omega_k$ . They can be computed as:

$$a_k = \frac{\frac{1}{w^2} \sum_{i \in \omega_k} u_I(i) u_p(i) - \mu_k \bar{p}_k}{\sigma_k^2 + \varepsilon} \quad (3)$$

$$b_k = \bar{p}_k - a_k \mu_k \quad (4)$$

Here,  $\mu_k$  and  $\sigma_k$  are the mean and variance of  $u_I$  in  $\omega_k$ , and  $\bar{p}_k$  is the mean of  $u_p$  in  $\omega_k$ .

However, a pixel  $i$  is involved in all the overlapping windows  $\omega_k$  that covers  $i$ , so the filtering output  $u(i)$  can be computed by:

$$u(i) = \bar{a}_i u_I(i) + \bar{b}_i \quad (5)$$

where  $\bar{a}_i = \frac{1}{w^2} \sum_{k \in \omega_k} a_k$  and  $\bar{b}_i = \frac{1}{w^2} \sum_{k \in \omega_k} b_k$  are the average coefficients of all windows overlapping  $i$ . More details and analysis can be found in [12].

We denote the Eq.(5) as  $u = \text{guidfilter}(u_I, u_p, w, \varepsilon)$ .

### 3. GUIDED IMAGE DECONVOLUTION

#### 3.1. Proposed Deconvolution Algorithm

Our algorithm is based on the decouple of deblurring and denoising steps in the restoration process.

In the **deblurring** step, we proposed two cost functions:

$$u_I = \arg \min_u \{ \lambda \| \nabla u - \nabla u_E \|_2^2 + \| h * u - y \|_2^2 \} \quad (6)$$

$$u_p = \arg \min_u \{ \lambda \| u - u_E \|_2^2 + \| h * u - y \|_2^2 \} \quad (7)$$

where  $u_E$  is a pre-estimated image, and  $\lambda > 0$  is the regularization parameter.

Alternatively, we diagonalized derivative operators after Fast Fourier Transform (FFT) for speedup. These yield solutions in the Fourier domain

$$\mathcal{F}(u_I) = \frac{\mathcal{F}(h)^* \cdot \mathcal{F}(y) + \lambda |\mathcal{F}(\nabla)|^2 \cdot \mathcal{F}(u_E)}{|\mathcal{F}(h)|^2 + \lambda |\mathcal{F}(\nabla)|^2} \quad (8)$$

$$\mathcal{F}(u_p) = \frac{\mathcal{F}(h)^* \cdot \mathcal{F}(y) + \lambda \mathcal{F}(u_E)}{|\mathcal{F}(h)|^2 + \lambda} \quad (9)$$

where  $\mathcal{F}$  is the FFT operator and  $\mathcal{F}(\cdot)^*$  denotes the complex conjugate.  $|\mathcal{F}(\nabla)|^2 = |\mathcal{F}(\partial_x)|^2 + |\mathcal{F}(\partial_y)|^2$  denotes the Fourier transform of  $\nabla$  operator. The plus, multiplication, and division are all component-wise operators.

To suppress the amplified noise and artifacts introduced by Eq.(9), in the **denoising** step, we applied the guided filter to smooth the estimated image  $u_p$ , and  $u_I$  is used as the guidance image. After the Fourier shrinkage steps [see Eq.(8) and (9)], the image  $u_p$  contains the more leaked noise and more details than  $u_I$ . So we use  $u_I$  as the guidance image and  $u_p$  as the filtering input image to recover some details and reduce the leaked noise.

The guided filter output is locally a linear transform of the guidance image. This filter has the edge-preserving smoothing property like the bilateral filter, but does not suffer from the gradient reversal artifacts. So we integrated this filter into the deconvolution problem. This leads to a powerful algorithm that produces high quality results.

Moreover, the guided filter has a fast and non-approximate linear-time algorithm, whose computational complexity is independent of the filtering kernel size. It has an  $O(N^2)$  time (in the number of pixels  $N^2$ ) exact algorithm for both gray-scale and color images.

We summarize the proposed algorithm as follows :

---

*Step 0:* Set  $k = 0$ , pre-estimated image  $u_E^k = 0$ , choose guided filter parameters  $w$  and  $\varepsilon$ .

*Step 1:* Use  $u_E^k$  to obtain the filtering input image  $u_p^k$  and the guidance image  $u_I^k$  with the Eq.(9) and Eq.(10), respectively.

*Step 2:* Apply guided filter to  $u_p^k$  with the guidance image  $u_I^k$ , and obtain a filtered output  $u^{k+1} = \text{guidfilter}(u_I^k, u_p^k, w, \varepsilon)$ .

*Step 3:* Set  $u_E^k = u^{k+1}$ , and  $k = k + 1$ .

*back to Step 1*

---

#### 3.2. Choose Regularization Parameter

Note that the Fourier-based regularized inverse operator in Eq.(8) and (9), and the deblurred images depend greatly on the degree of regularization which is determined by the regularization parameter  $\lambda$ . Now, we describe a simple but effective method to compute the parameters automatically.

Based on Morozov's discrepancy principle [13], which selects  $\lambda$  by matching the norm of the residual to some upper bound, a good regularized solution  $u$  should lie in the set  $\{u; \| h * u - y \|_2^2 \leq c^2\}$ , where  $c$  is a constant that depends on the noise level [14], we use the set  $\mathcal{K} = \{u; \| h * u - y \|_2^2 \leq \rho N^2 \sigma^2, 0 < \rho \leq 1\}$  in this work. By Parseval's theorem and Eq.(10)

$$\begin{aligned} \| h * u_p - y \|_2^2 &= \| \frac{\lambda(\mathcal{F}(h) \cdot \mathcal{F}(u_E) - \mathcal{F}(y))}{|\mathcal{F}(h)|^2 + \lambda} \|_2^2 \\ &\leq \| h * u_E - y \|_2^2 \end{aligned} \quad (10)$$

If the pre-estimated image  $u_E \in \mathcal{K}$ , we set  $u_I = u_p = u_E$ , and  $\lambda = \infty$ ; Otherwise, a proper parameter  $\lambda$  is chosen by

$$\| \frac{\lambda(\mathcal{F}(h) \cdot \mathcal{F}(u_E) - \mathcal{F}(y))}{|\mathcal{F}(h)|^2 + \lambda} \|_2^2 = \rho N^2 \sigma^2 \quad (11)$$

Notice that the left-hand side is monotonically increasing function in  $\lambda$ , hence there exist a unique solution  $\lambda$ , which can be determined via bisection.

From the Eq.(11), it is clear that the  $\lambda$  increases with the increase of  $\rho$ . Typically the value of  $\rho$  is set to 1 [14]. But in practice, we find that the large  $\lambda$  ( $\rho = 1$ ) often causes a noisy result with ringing effects, though it can substantially reduce the noise variances. So, we should choose a smaller  $\lambda$  ( $\rho < 1$ ) which would obtain an edge preserving image with less noise. Then, in the denoising step, our effective approach based on guided filter can be employed.

For a smooth image which contains a little high-frequency information, a large  $\rho$  will not produce the strong ringing effects and could substantially suppress the noise. That is to say, the parameter  $\rho$  should increase with the decrease of image variance. According to this property, we compute the  $\rho$  as follow:

$$\rho = \sqrt{1 - \frac{\|y - \mu(y)\|_2^2 - N^2 \sigma^2}{\|h\|_1^2 \|y\|_2^2}} \quad (12)$$

where  $\mu(y)$  denotes the mean of  $y$ .

#### 4. EXPERIMENTS RESULTS

The standard  $256 \times 256$  images *Cameraman* and *House* are tested in our experiments. The experiment settings are presented in Table.1. Table.1 describes the different point spread functions (PSF) and different amounts of white Gaussian additive noise.

In the experiments, we work on gray-scale images with intensity values normalized to the range  $[0,1]$ . Parameters  $\varepsilon$  and  $w$  of guided filter (in Eq.(3)) should be set carefully. For this work, we have just tried to evaluate how robust the algorithm behaves for two different images and a wide range of image degradations. For this purpose we have hand-optimized the two parameters for using them with five degradations and two images, obtaining  $\varepsilon = 7.5 \times 10^{-4}$  and  $w = 3$ .

We compare the proposed method with four state-of-the-art algorithms: ForWaRD [1], TVS [6], SV-GSM [7], L0-AbS [10] in standard test settings for deconvolution. Table.2 and Table.3 compared the results of our method and the other four methods in terms of ISNR (improvement in signal-to-noise-ratio). In our experiments, our method clearly outperforms the other four methods. In MATLAB simulation, we have obtained times per iteration of 0.098 seconds using  $256 \times 256$  image with an Pentium(R) Dual-Core CPU E5300 @2.60HZ and 2G RAM. The running time of the whole process (round 30 iterations) was 2.94s.

Fig.1 shows a visual comparison between the proposed method and the method in [10] on *Cameraman* image in test setting 3. Whereas both results recover the original image well, it is noticeable that our result preserves the edge better (see, the man's face). In Fig. 2 we compare to [6] on *House*

image in test setting 4. Our method recovers the sharpness of some edges (for instance, vertical edges in window) that in [6] are still blurry.

Tsets	PSF	$\sigma^2$
1	$h(i, j) = 1/(1 + i^2 + j^2)$ , for $i, j = -7, \dots, 7$	2
2	$h(i, j) = 1/(1 + i^2 + j^2)$ , for $i, j = -7, \dots, 7$	8
3	$h$ is a $9 \times 9$ uniform kernel (boxcar)	0.308
4	$h = [1 \ 4 \ 6 \ 4 \ 1]^T [1 \ 4 \ 6 \ 4 \ 1]/256$	49
5	$h$ is a Gaussian PSF with standard deviation 1.6	4

**Table 1.** Experiment settings with different blur kernels and different values of noise variance  $\sigma^2$  for pixel values in  $[0,255]$ .

Methods	Test 1	Test 2	Test 3	Test 4	Test 5
[1]	6.76	5.08	7.40	2.40	3.14
[6]	7.41	5.24	8.56	2.57	3.36
[7]	7.45	5.55	7.33	2.73	3.25
[10]	7.70	5.55	9.10	2.93	3.49
Our Method	<b>8.16</b>	<b>6.09</b>	<b>9.53</b>	<b>3.36</b>	<b>3.95</b>

**Table 2.** ISNR (in dB) of different methods on *Cameraman* image.

Methods	Test 1	Test 2	Test 3	Test 4	Test 5
[1]	7.35	6.03	9.56	3.19	3.85
[6]	7.98	6.57	10.39	4.49	4.57
[7]	8.64	7.03	9.04	4.30	4.11
[10]	8.40	7.12	10.74	4.55	4.80
Our Method	<b>8.83</b>	<b>7.46</b>	<b>11.11</b>	<b>4.84</b>	<b>5.34</b>

**Table 3.** ISNR (in dB) of different methods on *House* image.

In Fig.3, we plotted a few curves of different  $\lambda$  values obtained from Tests 2, 3 and 4 using *Cameraman* image, respectively. Hence, unlike some of the other deconvolution algorithms such as that in [5], our method automatically determines the regularization parameter at each iteration.

#### 5. CONCLUSION

We have presented a new deconvolution method based on guided image filtering. Guided filter is a novel explicit image filter. It has been proved to be more effective than the bilateral filter in several applications. We first integrate this filter into the deconvolution problem to propose an efficient iterative algorithm, which leads to highquality results. Through ten standard simulation experiments, it outperforms four existing state-of-the-art deconvolution algorithms. We find remarkable how such a simple method with just two parameters, compares favorably to other much more sophisticated methods. We also proposed a simple and effective method of automatically determining the regularization parameter at each iteration.



**Fig. 1.** Comparisons with *Cameraman* image in test setting 3. From left to right and from top to bottom: original image, blurred image, result from [10] (9.10 dB) and our result (9.53 dB).

## 6. REFERENCES

- [1] R. Neelamani, H. Choi, and R. G. Baraniuk, "ForWaRD: Fourier-wavelet regularized deconvolution for ill-conditioned systems," *IEEE Trans. Image Process.*, vol. 52, pp. 418-433, Feb. 2004.
- [2] J. Starck, M. K. Nguyen, and F. Murtagh, "Wavelets and curvelets for image deconvolution: A combined approach," *Signal Process.*, vol. 83, pp. 2279-2283, 2003.
- [3] V. M. Patel, G. R. Easley, and Dennis M. Healy, Jr, "Shearlet-Based Deconvolution" *IEEE Trans. Image Process.*, vol. 18, pp. 2673-2685, Dec. 2009.
- [4] H. Yang, Z. B. Zhang, "Fusion of Wave Atom-based Wiener Shrinkage Filter and Joint Non-local Means Filter for Texture-Preserving Image Deconvolution" *Optical Engineering.*, vol. 51, pp. 67-75, Jun. 2012.
- [5] Y. Wang, J. Yang, W. Yin, and Y. Zhang, "A new alternating minimization algorithm for total variation image reconstruction," *SIAM J. Imag. Sci.*, vol. 1, pp. 248-272, 2008.
- [6] O. V. Michailovich, "An Iterative Shrinkage Approach to Total-Variation Image Restoration." *IEEE Trans. Image Process.*, vol. 20, pp. 1281-1299, May. 2011.
- [7] J. A. Guerrero-Colon, L. Mancera, and J. Portilla, "Image restoration using space-variant Gaussian scale mixtures in overcomplete pyramids," *IEEE Trans. Image Process.*, vol. 17, pp. 27-41, Jan. 2007.
- [8] K. Dabov, A. Foi, V. Katkovnik, and K. Egiazarian. "Image restoration by sparse 3D transform-domain collaborative filtering." *Proc SPIE Electronic Image'08*. vol. 6812, San Jose, 2008.
- [9] R. Rubinstein, A. M. Bruckstein, and M. Elad, "Dictionaries for sparse representation modeling, *Proc. IEEE*, vol. 98, pp. 1045-1057, Jun. 2010.

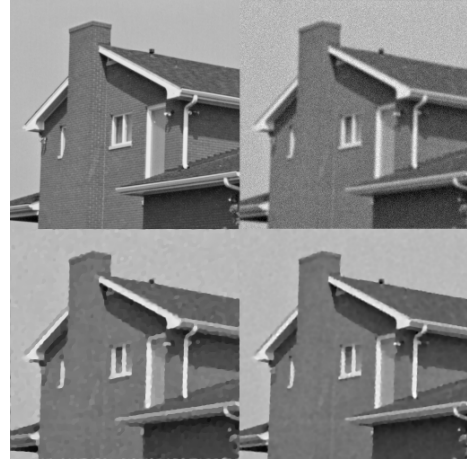


**Fig. 2.** Visual comparison of *House* image in test setting 4. From left to right and from top to bottom: original image, blurred image, result from [6] (4.49 dB) and our result (4.84 dB).

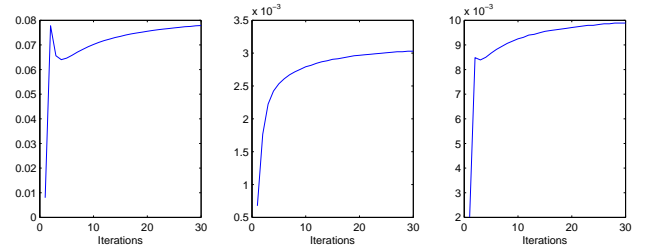


**Fig. 3.**  $\lambda$  values obtained by the method described in Eq.(11) using *Cameraman* image. From left to right: Test 2, Test 3, Test 5.

- [10] J. Portilla, "Image restoration through  $l_0$  analysis-based sparse optimization in tight frames," in *Proc. 16th IEEE ICIP*, Cairo, Egypt, pp. 3909-3912, 2009.
- [11] K. He, J. Sun, X. Tang: "Guided image filtering". In *Proc. of the European Conference on Computer Vision*, vol. 1, pp. 1-14, 2010.
- [12] K. He, J. Sun, X. Tang, "Guided Image Filtering", *IEEE Transactions on Pattern Analysis and Machine Intelligence*, accepted, 2012. Available online: <http://research.microsoft.com/en-us/um/people/kahe>.
- [13] S. Anzengruber and R. Ramlau, "Morozov's discrepancy principle for Tikhonov-type functionals with non-linear operators," *Inverse Problems*, vol. 26, pp. 1-17, 2010.
- [14] M. Ng, P. Weiss, and X. Yuan, "Solving constrained total-variation image restoration and reconstruction problems via alternating direction methods," *SIAM J. Sci. Comput.*, vol. 32, pp. 2710-2736, Aug. 2010.